Fast Inverse Forging Simulation via Medial Axis Transform

Philipp Blanke
Institute for Man-Machine-Communication
Leibniz Universität Hannover
Welfengarten 1, 30167 Hannover, Germany
blanke@gdv.uni-hannover.de

Franz-Erich Wolter
Institute for Man-Machine-Communication
Leibniz Universität Hannover
Welfengarten 1, 30167 Hannover, Germany
few@gdv.uni-hannover.de

Abstract

Hot metal forging and precision-forging of machine parts are important production techniques. Forging processes generally consist of several steps and have to be designed from top down. Beginning with the final product, the design engineer derives the intermediate steps of the process in inverse order, using simulations to evaluate and validate them. The simulations are generally based on the finite element method, a widely employed technique in engineering. Two problems exist with this method:

1. *The run-time of the simulations is often very long, depending on the spatial and temporal resolution of the simulated process.*
2. *The simulation progresses from one intermediate step to the next, while the engineer has to lay out the steps in inverse order.*

We propose a technique which adresses these problems, by following an approach relying on the geometry of the form and elementary plasticity theory. This method allows for a coarse approximation of the material flow that can be inverted.

1. Introduction

Forging is a resource-saving forming technique for highly stressed parts, that are, for example, used in safety critical positions. An important forging method is *hot metal drop forging* where a heated semi-finished part is placed between two forging dies that move towards each other. By pressing the upper forging die against the lower, a load is applied that increases the stress on the material until flow stress is reached and the material deforms plastically. Thus, the material fills the cavities of the dies, which capture the endform inversely. The quality of the final product depends on

- the (computer aided) tool construction and production;
- design of the forming stages;
- tolerances of the part;
- temperature control during the process (heat treatment);
- forging machine and used tools;
- automatization of the process.

Here, construction and design of the process is playing a key role. If the design of the forging dies or the layout of the process is incorrect, the quality of the final product will be severely reduced. Since the design of the tools is a very cost-intensive part of forging, computer aided techniques are used to reduce design time and to decrease the number of iterations until the final layout is reached. In particular, simulations of the forging process are conducted to gain reliable predictions for the material behavior and to guarantee that important parameters are met. The simulations are developed from equations of general plasticity theory, which are derived from general principles, such as conservation of mass or balance of linear and angular moments, and the constitutive description of the material.

Today, the most widely used approach for the prediction of flow patterns and temperature distribution during the forming process is the finite element analysis. The main role of the finite element method (FEM) is to verify the die designs that were accomplished by using empirical relationships or based on engineering practice. Usually, a number of pre-forms are needed in order to achieve the final complex shape from the initial simple shape with optimal properties and within a geometrical tolerance. The FEM is employed to find a solution of the partial differential equations (PDE) derived from general plasticity theory that describe the stress, strains, and material flow of the deformed medium dependent on temperature, deformation and friction.

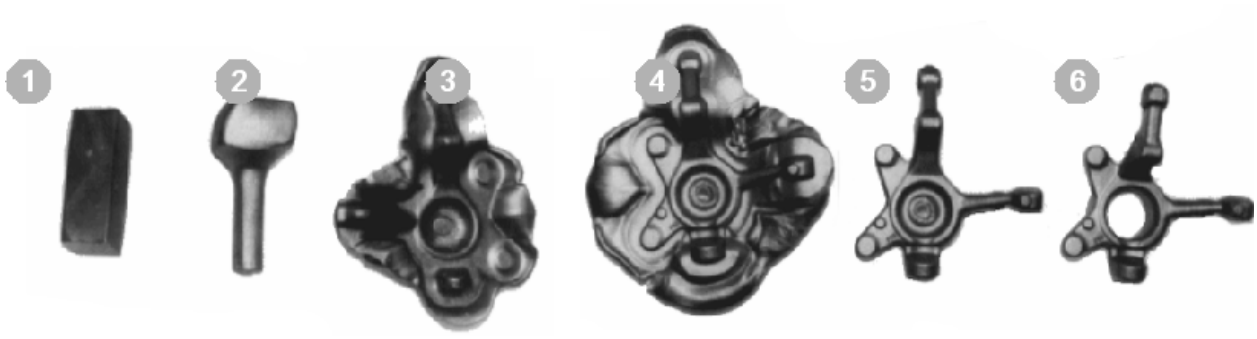

Figure 1. 1) cutting 2) pre-bulging 3) pre-forging 4) final forging 5) chamfering 6) punching

Simulations usually start with the non-deformed part and result in the final shape, while the engineer has the specifications of the final product and wants to derive the preform. Therefore, there exist several approaches today, towards inverse (or "backward") simulation of forging processes. The *backward deformation method* developed by Hwang et al. [11] and subsequently used by Biglari et al. [4] and others tries to invert the FEM simulation. Since a plastic deformation is – in contrast to elastic deformation – irreversible, the FEM simulation cannot be simply inverted, thus a backward tracking is employed. Here the velocity of nodes is predicted from timestep to timestep and iteratively compared with the result of forward simulation, taking advantage of an optimization to speed-up the costly iteration. The central problem faced in this approach is the contact of material with the die boundary. To solve the underlying equation, the material boundary has to be partitioned in free parts and parts where pressure/traction is applied. In the forward simulation approach, new contact comes naturally with the movement of the dies and deformation of the material. In the inverse direction, the loss of contact can not be predicted. Therefore different strategies have been implemented which solve the problem for specialized die forms.

Another type of algorithms are the 2.5 dimensional *upper bound element technique* (UBET) and 3-dimensional *tetrahedral upper bound analysis* (TEUBA) introduced by Bramley et al. [6]. Bramley subdivides the deforming region into elements of predefined types which are adapted to special configurations in the design of forging dies and thus limiting the range of possible forming geometries. Based on an upper-bound theorem by Prager and Hodge a limiting approach is pursued to predict the maximum energy and assure that the material is plastically deformed into a desired shape. Starting with an admissible velocity field that satisfies the incompressibility, continuity, and the velocity boundary conditions, the upper bound technique yields a velocity distribution by minimizing the total forming energy rate of the system with respect to the boundary velocities. The lower the computed upper bound is, the better the prediction.

These algorithms have quite severe drawbacks, since they have to be fitted closely to the problem at hand and have to our knowledge not been utilized in practical applications.

1.1. Dynamical system formulation

Plastic deformations of material are by nature irreversible problems. We try to find a simplified model, that can be inverted to give the engineer assistance in laying out the forming process. One approach would be to consider the problem of determining the material's velocity field by only looking at the velocity field of the material boundary. If the progression of the material front could be formulated as a dynamical system, one could try to invert the linearized system in a stepwise fashion. We will consider this approach in the future. In this paper we will look into the approach of displacement paths, as defined by Mathieu.

2. Displacement paths

As an alternative to FEM simulations Mathieu et al. proposed an approach based on experimental observation and elementary plasticity theory [13]. In drop forging experiments, Mathieu noticed that the material flow followed specific paths. He postulated that these could be locally described by a ball jammed between the dies which moves into the direction of least restraint when a load is applied to it by the moving tools. The center of this ball rolling inside the form and touching the die surface in at least two points will then trace the paths of material displacement. These paths are an application of the Medial Axis concept from geometric modeling, that we will review in more detail in section 2. For an example, refer to figure 2, where the simulation of a velocity field in a forging die is shown. Notice that the general direction of vectors is similar to the MA of the 2d cut through the tool shown in figure 3.

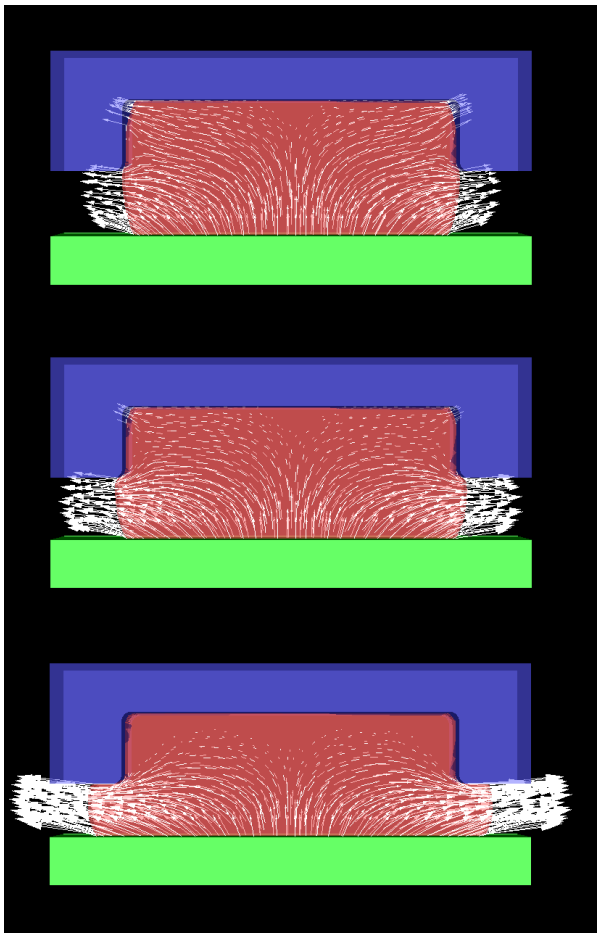

Figure 2. Simulation of the velocity field in a simple case. Shown are the upper and lower forging die, with the transformed material between them. The white arrows indicate velocity vectors of the material.

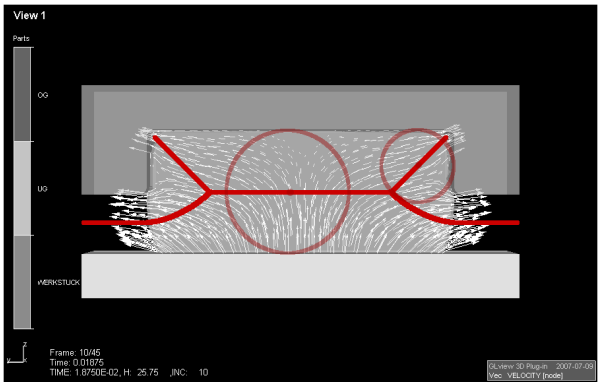

Figure 3. The Medial Axis of the die cavity with two maximal balls.

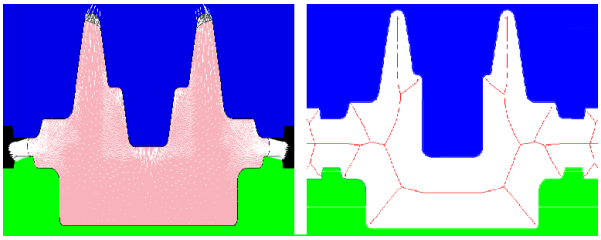

Figure 4. Two-dimensional example of a flow field and the MA of the die cavity.

Based on Mathieu's observations, an algorithm was developed which simulates the material transport along these displacement paths for rotationally symmetric parts, which can be described by a 2D cut [3]. The algorithm was generalized in [14] by a fuzzy logic approach for the material flow between two 2D cuts. It is important to note that the simulation will only provide an approximation to the velocity field of the material and the filling of the forging form. It will not yield local stresses, strains or temperature, and it does not allow for hardening phenomena. Thus, it can provide only limited assistance for the design of forging tools. But it seems that this approach is a good basis for a backwards simulation scheme. The displacement paths are only dependent on the a priori known geometry, and material transport will mainly follow them. Thus we have, in the case of hot forging, important information that gives rise to a new model of material transport, distinctly different from traditional approaches.

Wienstroer used the displacement path concept to develop a backwards simulation for the 2d case, appliable to rotationally symmetric shapes, see [15]. There, the problem of finding zones of tool-material contact is solved by partitioning the die cavity into cells depending on the displacement paths, computing the degree of filling, and determining the contact zone accordingly. The velocity field of the material is not computed explicitly, rather an iterative method based on flow resistance along the displacement paths is used to determine the distribution of material between the cells. An overview of the algorithm is given in section 4.

The algorithm presented here is based on the conventional rigid/ideally plastic formulation of the material. In the outlook we show, how the concept of Mathieu can be derived, if the material is regarded as a highly viscuos Bingham-fluid. In this article we want to present the problem and the progress we have made so far.

3. Medial Axis Transformation

The Medial Axis Transform (MAT) was introduced by Blum in 1967 as a tool for the description of the shape of biological objects [5]. Considering a reference object S, it consists of a subset of S - the Medial Axis (MA) - which can be thought of as a "skeleton" and a function defined on this skeleton which indicates the local "thickness" of the object. In the mathematical formulation, we will define the MA only for compact subsets of the Euclidean space, but it should be noted that more general definitions are possible, see ,e.g., [16] and [2] for a good review. In the following let S be a compact subset of the n-dimensional Euclidean space.

Definition 1 (Maximal Ball) *We call an n-dimensional ball $B_{c,r} \subset S$ with center $c \in \Re^n$ and radius r* maximal in S *if there exists no other ball $B_{c',r'} \subset S$ that contains $B_{c,r}$.*

Note that a maximal ball will either touch the border ∂S of S in at least two points or it is a ball of curvature with respect to ∂B.

Definition 2 (Medial Axis Transformation) *Let S be a compact subset of the $\Re^n$. The* Medial Axis M_S *of S is defined as the closure of centers of maximal n-balls relative to S. The* radius function $r : M_S \rightarrow \Re$ *assigns the radius of the corresponding maximal ball to every point in M_S.*

The points where the maximal ball around center $c \in M_S$ touches the boundary are called footpoints of c. For $n = 2$, the angle between the tangent to the MA at c and the path from c to either of its footpoints is called *medial angle* of c. We can categorize the points of the Medial Axis as shown by Giblin and Kimia in [9]:

- Curve points are points with exactly two footpoints.
- Vertex points are points with a finite number $n > 2$ of footpoints. Here, n curves will meet.
- Curve endpoints are points which are centers of curvature circles respective the boundary. This means there exist an infinite number of footpoints that form a continuous part of the boundary.

With this categorization a graph-structure can be built from the MA, see e.g. [8]. The vertices of the graph are the vertex points and the edges are the curves between them. The graph will have the same homotopy type as its reference set (see [16], [12]), it will particularly have the same connectivity and topology. In the case of a set homotopic to a sphere, the graph can not contain loops so it will in fact be a tree. These properties are important for the developed algorithm, since it is based on the tree structure of the MA.

The Medial Axis is closely related to the Voronoi diagram of a point set that is defined as follows.

Definition 3 (Voronoi diagram) *Given is a finite set of points $P = \{P_1, \ldots, P_n\} \subset \Re^n$ from the Euclidean n-space. Each point P_i can then be mapped to a* Voronoi cell V_i*, which is an open subset of $\Re^n$, so that for every point $q \in V_i$ the distance to P_i is less than to P_j. The subsets V_i together with the collection of their borders form a partition of $\Re^n$ which we call the* Voronoi diagram of P.

In two dimensions, the Voronoi diagram consists of line-segments (edges) bordering the convex Voronoi cells and meeting in so-called Voronoi points. In three dimensions, the Voronoi cells are bordered by convex planar facets and their edges. The borders of the Voronoi cells are equidistant to at least two points P_i. This observation leads to a relation with the Medial Axis of a set S. If the border of S is sampled with a certain sampling density σ, there is a subset of the Voronoi diagram of the sample that converges to the MA as σ increases as shown by Amenta et al. [1] and Dey et al. [7]. Therefore, it is possible to approximate the MA from the Voronoi diagram with a filter criterion that selects certain parts of the Voronoi diagram. This result is important, because the exact computation of the MA is tedious and in many applications an approximation to the MA is sufficient. The computation of the Voronoi diagram in contrast is well understood and readily available in a number of software packages.

In our work, we need the MA as a tool to compute an approximation to the material flow in hot forging. More precisely, we want to find flow paths on the medial surface, that means shortest paths between points on the MA. Therefore we need an approximation of the MA that conserves connectivity and should be within a bounded distance from the original. A fast approximation algorithm that fulfills these requirements is the algorithm of Dey et al. [7].

Since we have to compute the MA for every timestep, it is desirable to detect the parts of the MA that don't have to be recalculated. These are obviously the points which have footpoints on the same die part and whose associated medial ball does not intersect other die parts.

We are only interested in the final shape of the deformed material and neglect the influence of temperature and deformation history on the process, it is sufficient to look at the movement of the object's boundary.

4. Algorithm

The result of the elementary considerations together with the medial axis can be used to construct an algorithm that determines material flow. We will describe the important steps of the backwards 2D algorithm. For a comprehensive description refer to [15].

4.1. Setup

Input to the algorithm is the geometry of the tool, which is given by a point sample of a planar axial cut through the die surface. We assume that the material exhibits rigid–perfectly plastic behavior. We use a standard Cartesian coordinate system with orthogonal axes $\vec{x}, \vec{y}, \vec{z}$. The deformed volume has a constant thickness b in $\vec{z}$ direction, and we will the cut will be in the $\vec{x}, \vec{y}$ plane. Furthermore, we describe the material by its flow curve together with a working temperature[1] t and a constant friction coefficient μ. Finally we require the maximum speed of deformation $\dot{\phi}_{\max}$ during the process.

The first step is the approximation of the Medial Axis via the Voronoi diagram of the point set as described in section 2, that produces a connected tree of Voronoi edges and vertices. The die area is partitioned, so that each edge e of the tree corresponds to a cell C as shown in figure 6. This is another approach than the one found in [15], since the way cells are defined there (for each vertex instead of edge) will not result in a partitioning of the area. The union of all cells covers the material. Now, we determine the points where the border of the material, i.e., the material front, cuts the medial axis. At these points, which we call *end points*, material will be removed to fill the volume which will be freed when the dies move. The volume movement depends on resistance along the displacement paths, therefore we compute a forming resistance for each cell of the partition, based on the following consideration.

4.2. Forming Resistance

We look into a simple 2D configuration shown in figure 5, where a load is applied on a symmetric element of infinitesimal volume from two sides as shown in figure 5, and we want to derive a relation for the deformation resistance of this element. The force dF_{tot} works on both the top and the bottom side which form an angle α, respectively $-\alpha$ with the $\vec{x}$-axis. The height of the element at the left side is $h + 2dh$, and at the right side it is h. The width of the element is dx. The force dF can be decomposed into

$$dF = dF_n + dF_R = dF_x + dF_y,$$

[1]Here, we assume isothermal conditions without heat flow during the process.

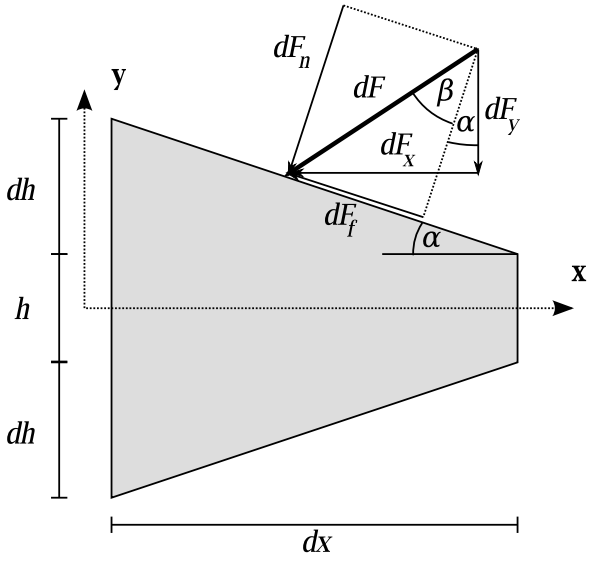

Figure 5. Simple configuration

where dF_n is the normal force on the top side arising if the contour slips with a friction force dF_R. The second equality describes the decomposition into forces in $\vec{x}$ and $\vec{y}$ direction.

With σ_x the stress on the left side and $\sigma_x + d\sigma_x$ the stress on the right side, we can express the force in $\vec{x}$ direction as

$$-2dF_x = -\sigma_x bh + \sigma_x(h + dh)b + d\sigma_x(h + dh)b \quad (1)$$

We have the geometric relation $dF_x = dF_y \tan(\alpha + \beta)$ and can express the force in $\vec{y}$ direction with the stress σ_y as $dF_y = |\sigma_y|\, dx\, b$. This gives the equilibrium equation

$$-\sigma_x bh + \sigma_x(h+dh)b + d\sigma_x(h+dh)b + 2|\sigma_y|\, dx\, b = 0. \quad (2)$$

Since b is a strictly positive constant, we can discard it from the equation, leaving

$$-\sigma_x h + \sigma_x(h + dh) + d\sigma_x(h + dh) + 2|\sigma_y|\, dx = 0. \quad (3)$$

If we assume that the material is plastically deformed, a yield criterion is fulfilled. Taking the criterion as stated by Tresca, we have $\sigma_{\max} - \sigma_{\min} = k_f$ where k_f is the flow resistance of the material. Since the strains in $\vec{x}$ direction are positive and those in $\vec{y}$-direction are negative and we neglect those in the $\vec{z}$ direction, the related stresses will also be positive, respectively negative and we get

$$\sigma_x - \sigma_y = k_f.$$

Inserting this in (3) and dividing by h and dx we have

$$\frac{d\sigma_x}{dx} + \frac{2}{h}\sigma_x(\tan(\alpha + \beta) - \tan\alpha) - \frac{2}{h}k_f \tan(\alpha + \beta) = 0. \quad (4)$$

This is an ordinary inhomogenous differential equation we will solve in the interval $[-h/2, h/2]$, with h denoting the width of the element. With $\mu = \tan(\alpha+\beta)$ and $\nu = \tan\alpha$, the general solution of the corresponding homogenous equation is

$$\sigma_x = c\,\exp(-\frac{2}{h}(\tan(\alpha+\beta)-\tan\alpha)(x+\frac{h}{2})).$$

where c is a constant. We define $A(x) := \exp((2/h)(\mu-\nu)(x+h/2))$, to get the special solution

$$\begin{aligned}\sigma_x &= A(x)^{-1}k_f \int_{-h/2}^{x} \frac{2}{h}\mu \\ &\quad \exp\left(\frac{2}{h}(\mu-\nu)(x+\frac{h}{2})\right)\,dx \\ &= k_f\frac{\nu}{\mu-\nu}\left(1-\exp(-\frac{2}{h}(\mu-\nu)(x+\frac{h}{2})\right)\end{aligned}$$

If we consider the special case where the two loaded sides are coplanar, i.e. $\alpha = \nu = 0$, so that $\mu = \tan\beta$, the equation simplifies to

$$\sigma_x = k_f\left(1-exp\left(-\frac{2}{h}\tan\beta(x+\frac{h}{2})\right)\right) \qquad (5)$$

We will interpret the resistance against the forming as the value of the mean normal stress $\bar{\sigma}_y$ in y-direction. Using the yield criterion of Tresca again, we get the following relation for the mean stresses

$$k_f = \bar{\sigma}_x - \bar{\sigma}_y \qquad (6)$$

We can compute $\bar{\sigma}_x$ by

$$\bar{\sigma}_x = \int_{-l/2}^{l/2}\frac{\sigma_x}{l}\,dx = k_f\left(1+\frac{h}{2l\tan\beta}\left(e^{\frac{-2l\tan\beta}{h}}-1\right)\right) \qquad (7)$$

Inserting (7) in (6) produces

$$\begin{aligned}\bar{\sigma}_y &= -k_f + k_f\left(1+\frac{h}{2l\tan\beta}\left(e^{\frac{-2l\tan\beta}{h}}-1\right)\right) \quad (8)\\ &= k_f\frac{h}{2l\tan\beta}\left(e^{\frac{-2l\tan\beta}{h}}-1\right) \quad (9)\end{aligned}$$

We see in this equation that the forming resistance for this simple configuration depends on the geometry – here the width and height – of the element.

To compute the forming resistance of the cell C, corresponding to the edge $E := v_1 - v_0$ between vertices v_0 and v_1 with footpoints f_0 and f_1[2] in distances r_0 and r_1. We substitute it by a simple element as shown in figure 6. We define the height of the substituted element to be $h := \bar{r}+\bar{r}'$, so that C has the same area as the quadrangle v_0, v_1, f_1, f_0. This yields

$$\begin{aligned}\bar{r} &= r_0\cos(\angle(E,(f_0-v_0)))|E| \\ &+ |f_0-f_1|\cos(\angle((f_0-f_1),(v_1-f_1))\,|v_1-f_1|\end{aligned}$$

and an equivalent expression for $\bar{r}'$. The width will then be $l = |E|$. Using (9) with μ as friction coefficient we get

$$\sigma_i = k_f\frac{|E|}{2(\bar{r}+\bar{r}')\mu}\left(e^{\frac{-4\bar{r}\mu}{|E|}}-1\right)$$

for the local deformation resistance of the cell.

Since the friction coefficient μ is given, the only unknown is the yield stress k_f that can be determined by a simplified Hensel-Spittel law

$$k_f = \gamma e^{m_1 T}\phi^{m_2}\dot{\phi}^{m_3}e^{\frac{m_4}{\phi}}$$

Here, γ is a material constant, $m_1,\ldots,m_4$ are the so called regression coefficients, ϕ is the degree of deformation and $\dot{\phi}$ the current deformation speed. The regression coefficients can be taken from tables or simulation programs such as FORGE and the deformation speed is specified by the user. That leaves the computation of the local maximum deformation degree $\phi_{\max}$ of each cell. Since the deformation will always be positive in the height and negative in the width of the cell, the deformation degree in the height is the maximal. When the movement vector of the die surface is s_D, and it forms an angle α with the vector $f_1 - f_0$, then the change of height dh will be

$$dh = s_D\sin(\alpha).$$

This yields

$$\phi_{\max} = \ln\left(\frac{h+s_D\sin(\alpha)}{h}\right).$$

With this result, we can compute the forming resistance of each cell.

4.3. Resistance along displacement paths

Since we assume that material will be transported along the MA, we still have to determine the volume ratios that are moved along the different branches. We postulate that the material will always move along the path of least resistance. Therefore, the total deformation resistance is added up along each branch of the MA and the displaced volume is distributed accordingly. To avoid multiple summation, the tree structure of the MA can be used to implement a backtracking algorithm, allowing fast computation of resistances for every vertex.

[2] We consider only one side of the cell, the other with footpoints f_0' and f_1' is treated equivalently.

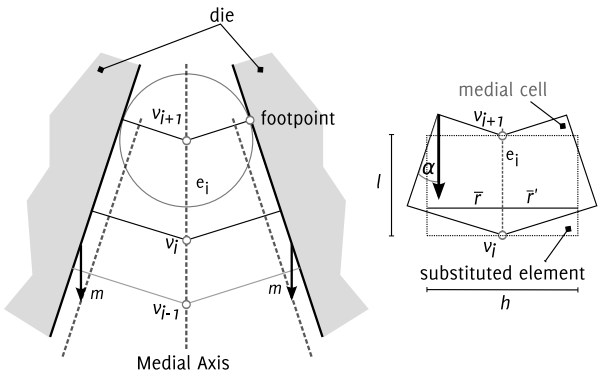

Figure 6. Cell and substituted element

Finally, the distribution of material volume will be calculated iteratively over the cells, depending on the determined resistances and a prescribed rate of transport, e.g., 5% of the volume per time-step. The latter rate is a heuristic, where further research could probably provide more transparent parameters.

We want to extend the simulation approach of Mathieu et al. to a real three-dimensional setting and to derive an inverse simulation scheme based on this approach. As the described algorithm will compute the volume transport in a two dimensional setting, several points have to be addressed:

- The approximation of the MA has to be conducted from the three dimensional Voronoi diagram, a starting point will be the algorithm by Dey et al. [7]. The arising partitioning will yield much more overhead managing the data structure.
- A concept of deformation resistance for three dimensional cells has to be developed.
- Flow paths have to be identified on the medial surface, ideally represented in a tree structure equivalent to the 2d case.

5. Fluid formulation and Outlook

In the following, we consider several important results from rheology, to illustrate the concept of displacement paths from a theoretical point of view. For laminar flow of a homogenous viscous fluid through a pipe, the law of Hagen-Poiseuille states for the volume flow $\dot{V}$

$$\dot{V} = \frac{\pi r^4 \Delta p}{8\eta l}$$

with η the dynamic viscosity of the fluid which captures its resistance to deform under shear stress. It can be seen that the resistance to flow depends strongly on the radius of the pipe, which goes into the equation to the power of four. The law is a special case of the Navier-Stokes equations and can also be stated for a rectangular cross-section with width w and height h:

$$\dot{V} = \frac{\Delta p \min(b,h)^2 bh}{K\eta l}$$

The constant K is from the interval $12 < K < 28.45$ and can be approximated by a formula given in [10].

The flow profile of the volume has the shape of a parabola with its maximum at the central axis of the pipe, which is identical to its Medial Axis. This confirms Mathieu's conjecture, since here the fluid moves fastest, so it will be the main flow path in this very simple example with a Newtonian fluid.

The above equation of Hagen-Poiseuille is not valid for non-Newtonian fluids, but it can be used for Bingham fluids, that are characterized by

$$\frac{\partial u}{\partial y} = \begin{cases} 0, & \tau < \tau_0 \\ (\tau - \tau_0)/\mu, & \tau \geq \tau_0 \end{cases}$$

These fluids behave like a rigid body, unless the shear stress is greater than the yield stress τ_0. Then they start to flow like Newtonian fluids. Thus, if stress is higher than the yield stress everywhere, the material's flow can be described by the Hagen-Poiseuille equation. Since in hot forging, the considered material is in a plastic regime, i.e., it can be viewed as a fluid with high viscosity, the above equations could be used to determine flow resistance. From this point of view one can argue for the conjecture of Mathieu by noticing that for straight parallel uniform flow in x-direction, shear stress τ between layers within the material can be formulated as

$$\tau = \eta \frac{\partial v}{\partial y}.$$

Thus, τ is proportional to the velocity gradient perpendicular to the layers, i.e., the relative motion of the layers. Now, if we consider multiple offsets of the die surface with distance ϵ, these surfaces can be interpreted as layers in which a point p of material will move, if there is already material-die contact at the point q_p. Here q_p shall be the point on the die surface, where a shortest path to p starts. The MA of the die gap is the set where the distance function from the boundary is not continuously differentiable anymore and therefore represents the collection of offset surfaces. Additionally points on the MA are locally farthest away from the boundary, so that the inner friction of material will be a local minimum.

We will look into these interesting connections which should lead to a better understanding of the flow phenomena

during the forging process. We will also address the points necessary for the development of a three dimensional version of the algorithm mentioned at the end of section 4.

6. Acknowledgements

This project is a collaboration with Prof. B.-A. Behrens and Dipl.-Ing. Hans Conrads from the Institute of Metal Forming (Institut für Umformtechnik) at the Leibniz University of Hannover; it is sponsored with a research scholarship from the Graduate College 615 of the German Research Foundation (Deutsche Forschungsgemeinschaft, DFG).

References

[1] N. Amenta and R. K. Kolluri. The Medial Axis of a Union of Balls. *J. Computational Geometry*, 20:25–37, 2001.

[2] D. Attali, J.-D. Boissonnat, and H. Edelsbrunner. Stability and Computation of Medial Axes: a State of the Art Report. In B. H. T. Möller and B. Russell, editors, *Mathematical Foundations of Scientific Visualization, Computer Graphics, and Massive Data Exploration*. Springer-Verlag, Mathematics and Visualization, 2004.

[3] W. Beneker. Rechnergestützte Simulation des Füllverhaltens beim Gesenkschmieden. *Fortschritt-Berichte VDI Reihe*, 20(187), 1995.

[4] F. Biglari, N. O'Dowd, and R. Fenner. Optimum design of forging dies using fuzzy logic in conjunction with the backward deformation method. *International Journal of Machine Tools and Manufacture*, 38(8):981–1000, August 1998.

[5] H. Blum. A Transformation for Extracting New Descriptors of Shape. In W. Wathen-Dunn, editor, *Proc. Models for the Perception of Speech and Visual Form*, pages 362–380. MIT Press, November 1967.

[6] A. Bramley. UBET and TEUBA: fast methods for forging simulation and preform design. *Journal of Materials Processing*, 116, 2001.

[7] T. K. Dey and W. Zhao. Approximating the Medial Axis from the Voronoi Diagram with a Convergence Guarantee. *Algorithmica*, 38:179–200, 2004.

[8] F. Fol-Leymarie. *Three-Dimensional Shape Representation via Shock Flows*. PhD thesis, Division of Engineering, Brown University, USA, 2003.

[9] P. J. Giblin and B. B. Kimia. On the Local Form and Transitions of Symmetry Sets, Medial Axes, and Shocks. *Int. J. of Computer Vision*, 54(1/2/3):143–157, 2003.

[10] J. P. Hartnett and M. Kostic. Heat Transfer to Newtonian and Non-Newtonian Fluids in Rectangular Ducts. *Advances in Heat Transfer*, 19:247–356, 1989.

[11] S. Hwang and S. Kobayashi. Preform Design in Disk Forging. *International journal of machine tool design & research* , 26(3):231–243, 1986.

[12] A. Lieutier. Any Open Bounded Subset of $\Re^n$ has the same Homotopy Type than its Medial Axis. In *SM '03, Seattle, Washington, USA*, June 2003.

[13] H. Mathieu. Ein Beitrag zur Auslegung der Stadienfolge beim Gesenkschmieden mit Grat. *Fortschritt-Berichte VDI-Reihe 2*, 213, 1991.

[14] M. Michael. *Konstruktionsbegleitende Modellierung von Schmiedeprozessen*. PhD thesis, Leibniz Universität Hannover, 1999.

[15] M. Wienströer. *Konstruktionsintegrierte Prozessimulation der Stadienfolge beim Schmieden mittels Rückwärtssimulation*. PhD thesis, Leibniz Universität Hannover, 2004.

[16] F.-E. Wolter. Cut Locus and Medial Axis in Global Shape Interrogation and Representation. *MIT Sea Grant Report*, 1992.